https://doi.org/10.5194/egusphere-2026-2204
Preprint. Discussion started: 23 April 2026

ESR-thermochronometry of the MIZ1 borehole, Tono, Japan

Georgina E. King[1]*, Lily Bossin[1,2], Maxime Bernard[1], Melanie Kranz-Bartz[1,3], Xiaoxia Wen[1], Christoph Schmidt[1], Benny Guralnik[1], Frédéric Herman[1], Manabu Ogata[4], Shigeru Sueoka[4]

[1]Institute of Earth Surface Dynamics, University of Lausanne, Switzerland.
[2]Paul Scherrer Institute, Villigen, Switzerland.
[3]Institute of Geosciences, Ruhr-University Bochum, Germany.
[4]Tono Geoscience Center, Japan Atomic Energy Agency, Toki, Japan.

Correspondence to: Georgina E. King (georgina.king@unil.ch)

Abstract. The electron spin resonance (ESR) of quartz can be used as a low temperature thermochronometric system, however, to date no field validation of the approach has been made. Here we explore the ESR signals of quartz from six samples from the MIZ1 borehole (Tono, Japan). Previous studies have shown that this low-relief region underwent Quaternary exhumation at rates of <0.2 mm yr^{-1}. We investigate whether quartz ESR signals can resolve such low rates of exhumation, or whether the samples are in thermal equilibrium with ambient borehole temperature. ESR thermochronometry requires that both sample-specific signal saturation and thermal decay are constrained in the laboratory, which makes measurements highly time-consuming. To overcome this, the development of a standardised growth curve (SGC) was explored, which allowed more rapid constraint of the trapped-charge concentrations of each of the samples. Thermal kinetic parameters were determined using an isothermal decay experiment for each individual sample and except for sample MIZ1-08, it was possible to fit all the isothermal decay data together to yield a single set of kinetic parameters that successfully described the dataset. The ESR thermochronometry results show that the MIZ1 samples are in thermal equilibrium for the Al-centre, and that Monte-Carlo inversion of the ESR data yields present-day borehole temperature within 1σ uncertainties for all samples except the lowest temperature sample. In contrast, inversion of the different Ti-centre options (A, B, D) yields temperatures 15-20 °C above contemporary borehole temperature, indicating rock cooling equivalent to a total exhumation of ~1 km over the same period. The cause of this discrepancy is unclear but may relate to sub-linearity of Ti-centre dose response, that led to underestimation of the trapped-charge concentration and hence an overestimation of borehole temperature. Our results validate ESR-thermochronometry of the Al-centre and show that an SGC and common thermal kinetic parameters may be used to expediate sample measurements, however ESR-thermochronometric data from the Ti-centre should be used cautiously until further validation data are available.

https://doi.org/10.5194/egusphere-2026-2204
Preprint. Discussion started: 23 April 2026

1 Introduction

Electron spin resonance (ESR) dating of quartz minerals offers a considerable advantage over luminescence dating because of its signal saturation at higher doses. We seek to exploit this to build upon previous studies in the development of a thermochronometry system capable of resolving rock cooling rates throughout the Quaternary. Thermochronometric techniques measure the evolution of rock temperature throughout time, that occurs as a result of rock uplift and exhumation. These techniques can thus be used to help understand landscape evolution in response to Earth surface processes. Whereas the luminescence thermochronometry system is limited to areas experiencing very rapid rock exhumation (and the associated cooling) of tens of mm yr^{-1} (e.g. Wu et al., 2015; King et al., 2016), previous studies indicate that ESR thermochronometry can resolve rates of <1 mm yr^{-1} over Quaternary timescales (e.g. Grün et al., 1999; Bartz et al., 2024; Wen et al., 2024). ESR-thermochronometry thus has the potential to provide constraint of rates of landscape evolution over timescales of ka-Ma, for rock cooling at temperatures <100 °C, a timescale and temperature range that remains elusive to most existing low-temperature thermochronometric systems.

A key challenge in the establishment of ESR-thermochronometry as a robust technique is finding data against which to benchmark results. This is because the method resolves a time and temperature period inaccessible to most other thermochronometers, either because of their higher closure temperatures, or because the low accumulation of daughter products over ka timescales leads to imprecise age estimations (e.g. accumulation of helium in apatite helium dating). ESR measurements of rock samples from boreholes can alleviate this challenge, because the final (modern day) ambient temperature of the rock is constrained. For this reason, we focus on six samples from the MIZ1 borehole, Tono, Japan (Uozumi et al., 2005), for which existing thermochronometric data are available (Yuguchi et al., 2017; Ogata et al., 2022). The Tono region is a low-relief zone that has remained stable throughout the Quaternary period and prior thermochronometric work indicates that the MIZ1 borehole has experienced exhumation at rates of <0.16 mm yr^{-1} (Yuguchi et al., 2017) over the past 40 Ma. The temporal and thermal limits of the ESR-thermochronometry system are poorly known, and thus in this study, we explore the application of ESR-thermochronometry to the MIZ1 borehole to investigate whether samples are in field-saturation with ambient temperature or rather yield exhumation rates of <0.2 mm yr^{-1}, consistent with previous data.

2 Study area and samples

The Tono district of central Japan is characterised by the remnants of uplifted peneplains known as the Mikawa and Mino Plateaus. These plateaus comprise depositional surfaces of the Toki sand and gravel formation (e.g. Moriyama and Niwa, 1985) and are thought to have been deposited during the Pliocene to early Pleistocene. The MIZ1 borehole (35°22’45.2131”N, 137°14’17.6964”E, 206.5 m a.s.l.; Uozumi et al., 2005) is located on the Mino plateau and was drilled by the Japan Atomic Energy Agency in 2003. It has a total length of 1300 m, but due to a slight subvertical inclination over the deepest 356 m

https://doi.org/10.5194/egusphere-2026-2204
Preprint. Discussion started: 23 April 2026

(Uozumi et al., 2005), has a true vertical depth of 1278 m. Sample locations are expressed as true vertical depth. The borehole lithology ranges from post-Paleogene sediments (0-109 m), hornblende-biotite granite facies of the Toki granite (109-508 m) to biotite granite facies of the Toki granite (508-1278 m).

Exhumation and uplift rates in this region have been determined using low temperature thermochronology (Yuguchi et al., 2017; Ogata et al., 2022), as well as through the dating of alluvial terraces (Tajikara et al., 2011). Yuguchi et al. (2017) used apatite fission-track dating obtaining an exhumation rate of $<0.16 \pm 0.04$ mm yr^{-1} of the Cretaceous Toki granitic pluton, over the past 40 Ma. These rates are consistent with uplift rates estimated between MIS 6 and 2 of 0.11–0.16 mm yr^{-1}, determined from a combination of radiocarbon dating, tephrochronology and pollen analyses of alluvial terraces along the Tokigawa river basin (Tajikawa et al., 2011). They are also consistent with recently measured OSL-thermochronometry data on six granitic samples at 159, 447, 742, 1027, 1178, and 1265 m depth from the MIZ1 borehole (Ogata et al., 2022). Ogata et al. (2022) found that their OSL-thermochronometry data were in field saturation with ambient borehole temperature, indicative of a low rate of rock exhumation.

The samples of Ogata et al. (2022) have estimated temperatures ($T_{\text{in-situ}}$) ranging from 22.7 to 43.8 ºC (Table 1) based on the ambient geothermal gradient of ~19 ºC km^{-1} (Hama et al., 2016) calculated from direct borehole temperature measurements in 2003 and 2004 (Uozumi et al., 2005). At the time of the temperature measurements, fluid in the borehole was observed to have a temperature lower than the host rock, resulting in both negative and positive temperature excursions, the latter occurring where fluid concentrations were reduced (Uozumi et al., 2005). Whilst borehole temperatures were found to be more stable below 200 m depth, a difference of up to ~2 °C was observed between temperature measurements at a depth of ~975 m (Uozumi et al., 2005). Drilling boreholes can result in modification of the geothermal gradient, and borehole temperatures are sensitive to surface temperature fluctuations (e.g. Pollack, 1993; Kohl, 1998; Bodri and Cermak, 2011). However, Ogata et al. (2022) calculated a palaeo-geothermal gradient from their IR_{100} OSL-thermochronometry data of 19.5 ºC km^{-1}, with a surface temperature value (T_0) of 19.5 ºC that is commensurate with modern-day in-situ temperatures, valid over ~0.1 Ma. In this study, we apply ESR-thermochronometry (Scherer, 1993; Grün et al., 1999; Fang and Grün, 2020; King et al., 2020) to the same sample set as Ogata et al. (2022), to explore whether ESR signals are also in thermal equilibrium with the ambient borehole temperature, or whether they are able to constrain very low rates of rock exhumation.

3 Methods

3.1 Sample preparation

Sample preparation followed standard methods for trapped-charge thermochronometry and is described in Ogata et al (2022). The exterior of the samples was removed using a diamond-saw under subdued red lighting before the light-safe interior was crushed by hand to extract the 180–250 µm fraction, which was treated with HCl and H_2O_2 to remove carbonates and any

https://doi.org/10.5194/egusphere-2026-2204
Preprint. Discussion started: 23 April 2026

organic material respectively. This fraction was then density separated to isolate heavy minerals >2.70 g cm^{-3} from quartz and feldspar minerals and the quartz enriched fraction (2.62-2.70 g cm^{-3}) was etched with 40 % HF for 40 min to remove contaminating feldspar minerals. The etched fraction was treated with HCl for 60 min to remove any fluorides that may have precipitated during HF etching and was sieved to >63 µm to remove any partially dissolved quartz grains. 60 mg aliquots of quartz were loaded into glass ESR sample tubes of 3 mm outer diameter and 2 mm inner diameter for measurement.

3.2 ESR Measurements

All ESR measurements were made at the University of Lausanne using a Bruker Magnettech ESR5000 X-band (~9.5 GHz) ESR spectrometer with a high-sensitivity resonator (TE102 rectangle) and a TCH04 liquid nitrogen temperature controller system that allowed measurement at 100 ± 1 K. Samples were positioned in the centre of the cavity and were measured three times following 120° rotation to compensate for any anisotropic effects of the quartz minerals (Preusser et al., 2009). The ESR signals of the Al and Ti centres were measured in a single spectrum at 10 mW microwave power, 100 kHz modulation frequency, 0.1 mT modulation amplitude, 40 mT sweep width (320-360 mT), 120 s sweep time and a single scan. All measured spectra were baseline corrected using the automatic baseline correction option in the ESR Studio software. Al-signals were determined from the peak-to-peak intensity of the top of the first peak to the bottom of the 16th peak (Toyoda and Falguères, 2003), whilst Ti-signals were determined using options A, B and D of Duval and Guilarte (2015).

3.2.1 Measurement of the trapped-charge concentration

To make an ESR-thermochronometry measurement, it is first necessary to constrain the trapped-charge concentration of each of the samples by measuring a dose response curve. Dose response curves were constructed using a single-aliquot regenerative dose (SAR) protocol following Tsukamoto et al. (2015), whereby aliquots were annealed at 400 °C for 4 min following measurement of the natural signal, before the addition of regenerative doses. Irradiation was done using a Freiberg Instruments X-ray irradiation unit with a calibrated dose rate of 0.206 ± 0.005 Gy s^{-1} (Bossin and King, 2021). Most aliquots measured using the SAR protocol were given a maximum accumulated dose of 2 kGy which was sufficient to constrain the equivalent dose (D_e) value of both the Al and Ti centres. Two aliquots of sample MIZ1-08 were irradiated into saturation which occurred at ~60 kGy for the Al-centre and ~7 kGy for the Ti-centre.

Tsukamoto et al. (2015) proposed that aliquots should be preheated prior to measurement. Following King et al. (2020) we selected a preheat treatment of 160 °C for 4 min. We tested whether this was appropriate by contrasting the D_e values obtained for preheated and non-preheated aliquots of samples MIZ1-08, MIZ1-09 and MIZ1-10 measured using a SAR protocol. None of the aliquots were preheated before measurement of the natural signal and all aliquots were subjected to an annealing step of 400 °C for 4 min following measurement of the natural signal.

https://doi.org/10.5194/egusphere-2026-2204
Preprint. Discussion started: 23 April 2026

Table 1: Sample details and kinetic parameters. $T_{in\text{-}situ}$ is the modern-day borehole temperature (Uozumi, 2005). $\dot{D}$ is the environmental dose rate; values from Ogata et al. (2022) were recalculated for quartz minerals using DRAC v.1.2 (Durcan et al., 2015), the conversion factors of Guérin et al. (2011), the beta grain size attenuation factors of Guérin et al. (2012) and the alpha grain size attenuation factors of Bell (1980, see Supplementary Material). s is the frequency factor, $\mu(E_t)$ is trap depth, $\sigma(E_t)$ is the width of the Gaussian trap distribution (Lambert, 2018) and D_0 is the characteristic dose of saturation calculated using a standardised growth curve (SGC) for all samples (see section 3.1). PH indicates that the aliquot was preheated, ages are calculated from the SGC using a fit truncated at 4.5 kGy (see section 3.1).

Al-centre	Depth (m)	$T_{in\text{-}situ}$ (°C)[1]	$\dot{D}$ (Gy ka^{-1})	$\log_{10}(s)$ (s^{-1})	$\mu(E_t)$ (eV)	$\sigma(E_t)$ (eV)	D_0 (Gy)	nNnat (no PH)	nNnat (PH)	Age (ka) (no PH)	Age (ka) (PH)
MIZ1-01	159	22.7 ± 1.72	6.28 ± 0.51	11.78 ± 1.42	1.39 ± 0.13	0.12 ± 0.02		0.124 ± 0.005	-[2]	549 ± 67	-[2]
MIZ1-03	449	28.2 ± 1.07	6.19 ± 0.47	12.18 ± 0.69	1.44 ± 0.06	0.14 ± 0.01		0.098 ± 0.002	0.124 ± 0.002	364 ± 32	559 ± 49
MIZ1-05	751	33.8 ± 0.81	5.90 ± 0.49	11.93 ± 0.53	1.43 ± 0.05	0.13 ± 0.01		0.080 ± 0.002	0.082 ± 0.000	284 ± 23	297 ± 26
MIZ1-08	1043	39.2 ± 0.81	5.54 ± 0.50	11.40 ± 0.65	1.43 ± 0.06	0.14 ± 0.01		0.065 ± 0.002	0.085 ± 0.000	230 ± 23	329 ± 27
MIZ1-09	1198	42.1 ± 0.81	6.14 ± 0.47	12.66 ± 1.09	1.48 ± 0.10	0.10 ± 0.01		0.033 ± 0.001	0.042 ± 0.001	92 ± 9	123 ± 11
MIZ1-10	1287	43.8 ± 0.81	7.10 ± 0.55	11.52 ± 1.18	1.37 ± 0.11	0.12 ± 0.01		0.053 ± 0.001	0.063 ± 0.001	139 ± 12	170 ± 14
All (excl. MIZ1-08)				12.10 ± 0.49	1.43 ± 0.04	0.12 ± 0.01	29,973 ± 1404				
Ti-centre – Option D											
MIZ1-01	159	22.7 ± 1.72	6.28 ± 0.51	12.16 ± 1.57	1.43 ± 0.14	0.12 ± 0.02		0.058 ± 0.004	-[2]	47 ± 4	-[2]
MIZ1-03	449	28.2 ± 1.07	6.19 ± 0.47	11.68 ± 0.84	1.40 ± 0.08	0.12 ± 0.01		0.048 ± 0.003	0.049 ± 0.004	39 ± 4	40 ± 4
MIZ1-05	751	33.8 ± 0.81	5.90 ± 0.49	12.36 ± 0.63	1.47 ± 0.06	0.13 ± 0.01		0.034 ± 0.007	0.060 ± 0.007	27 ± 4	49 ± 5
MIZ1-08	1043	39.2 ± 0.81	5.54 ± 0.50	11.71 ± 0.79	1.42 ± 0.07	0.10 ± 0.01		0.030 ± 0.007	0.030 ± 0.013	30 ± 3	24 ± 3
MIZ1-09	1198	42.1 ± 0.81	6.14 ± 0.47	11.19 ± 1.33	1.36 ± 0.12	0.10 ± 0.02		0.021 ± 0.004	0.025 ± 0.007	17 ± 2	20 ± 4
MIZ1-10	1287	43.8 ± 0.81	7.10 ± 0.55	11.81 ± 1.16	1.40 ± 0.10	0.12 ± 0.01		0.023 ± 0.006	0.021 ± 0.010	18 ± 3	17 ± 3
All (excl. MIZ1-08)				11.81 ± 0.53	1.41 ± 0.05	0.12 ± 0.01	3,879 ± 165				

[1]Uncertainties (1σ) are estimated from the deviation between four borehole temperature measurements made in 2003 and 2004 (Uozumi, 2005); as only one temperature measurement was made for samples >1 km depth, the uncertainty is estimated from the overlaying sample.

[2]Aliquot lost during analysis.

A potential disadvantage of SAR measurement protocols is that sensitivity change may occur following the 400 °C for 4 min annealing of aliquots after measurement of the natural signal (e.g. Grün et al., 1999). To test whether the samples were affected by sensitivity change, an aliquot of samples MIZ1-08, MIZ1-09 and MIZ1-10 was also measured using a single aliquot additive dose (SAAD) method. Aliquots were not annealed after measurement of the natural signal before construction of the dose response curve and were preheated at 160 °C for 4 min before measurement following each additive dose (maximum added dose 62 kGy). Finally, a dose-recovery test was carried out using two aliquots each of samples MIZ1-01 and MIZ1-08, that

https://doi.org/10.5194/egusphere-2026-2204
Preprint. Discussion started: 23 April 2026

were annealed for 90 min at 400 °C prior to irradiation with 1,030 Gy and measurement in a SAR protocol either with or without preheating.

3.2.2 Measurement of thermal stability

The thermal stability of the different samples was measured using an isothermal decay experiment (e.g. King et al., 2020), whereby four aliquots of each sample were annealed at 400 °C for 30 min prior to irradiation with a dose of 1,030 Gy. Each aliquot was then preheated at 160 °C for 4 min before being annealed using one of the following temperatures, 130 °C, 160 °C, 200 °C and 250 °C, for various durations ranging from 4 min up to a cumulative duration of 10 h.

4 Results

4.1 Trapped-charge concentrations

All samples investigated yielded ESR signals of sufficient intensity to allow precise measurements (Fig. S1). The natural non-normalised signal intensities of the different samples reduce with increasing borehole temperature (Fig. 1). Where multiple aliquots were measured for individual samples, some scatter is observed for some signals, e.g. for Ti-centre option A (Fig. 1c).

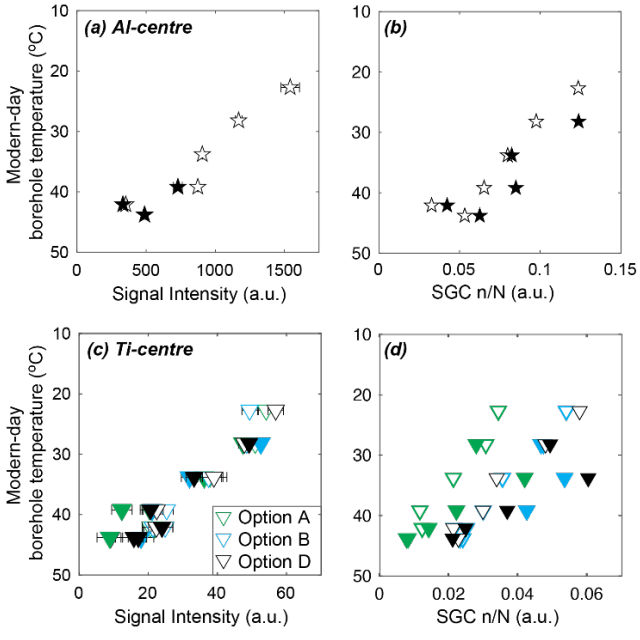

Figure 1: Signal intensity and fraction of saturation (n/N) variation with borehole temperature for the (a,b) Al- and (c,d) Ti-centres of the different samples (see Table 1). Filled symbols indicate aliquots that were preheated. n/N values have been calculated from a standardized growth curve (SGC), see text for details.

Dose response curves were fitted using both a single (SSE) and double saturating exponential (DSE) function, no data weighting was used for model fitting (Fig. S2). Equivalent dose values were determined from interpolation onto the SAR dose

https://doi.org/10.5194/egusphere-2026-2204
Preprint. Discussion started: 23 April 2026

response curves (Table S1). Individual D_e value uncertainties for the Al-centre were <8 % for the SSE fit, and <6 % for the DSE fit, whilst D_e values obtained with the different fits differ by ≤5 %. In contrast, the dose response of all Ti-signals was somewhat sub-linear (Fig. S.2B) and was not well described by either an SSE or DSE fit, both fit types yielded relatively high uncertainties. Individual D_e value uncertainties for Ti-centre option D range from 2-16 % for both fits, but uncertainties are greater for options A and B. Equivalent dose values obtained using either fit differ by <0.05 %. Different aliquots (n=2) of the same sample have D_e values that vary by 15-39 % for the Al-centre and 4-68 % for the different Ti-centre options. Preheated aliquots have a lower D_e for the Ti-centre, but no trend is observed for the Al-centre.

To confirm the suitability of our measurement protocol, a dose-recovery test was done using two aliquots of two samples; one aliquot of each sample was preheated, whilst the other aliquot was not preheated. All dose-recovery measurements yield dose-recovery ratios within 15% of unity (Table S3), although one of the preheated aliquots was lost during measurement. These results imply that the selected measurement protocol is appropriate, and that the samples are not suffering significant sensitivity change between measurement of the natural and regenerative doses. A further investigation of potential sensitivity change was made through contrasting the SAAD and SAR measurements of three samples.

To contrast the SAAD and SAR dose response curves, the D_e values determined from the sample specific SAR dose response curves were added to the SAAD given dose values, and the data plotted together (Fig. 2). In the absence of sensitivity change, the SAAD and SAR dose response curves should then overlay one another (e.g. Grün et al., 1999; Fang and Grün, 2020; Wen et al., 2024), which is the case for both the Al and Ti centres of the three samples investigated, MIZ1-08, MIZ1-09 and MIZ1-10 (Fig. 2, Fig. S3-4), irrespective of aliquot preheating. Equivalent dose values are broadly consistent (within ~20 %) between SAAD and SAR fits (Fig. S5), providing that only the initial part of the SAAD dose response curve is fitted for curve extrapolation, i.e. <4.5 kGy.

https://doi.org/10.5194/egusphere-2026-2204
Preprint. Discussion started: 23 April 2026

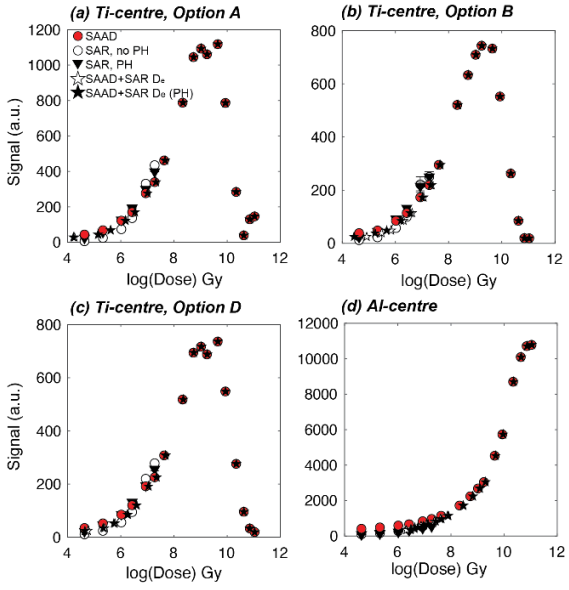

Figure 2: Comparison between SAR and SAAD dose response curves measured for different aliquots of sample MIZ1-09 for the Ti-centre (a) option A, (b) option B, (c) option D and (d) the Al-centre.

In addition to good agreement between SAR and SAAD dose response curves for the same sample, dose response appears to be similar between samples, therefore the potential of a standardised growth curve (SGC) was investigated. An SGC would offer the advantage that not all aliquots would need to be dosed until saturation, which occurs at ~7 kGy and ~60 kGy for the Ti- and Al-centres of these samples respectively. The SAAD dose response data for samples MIZ1-09 and MIZ1-10 are almost identical (Fig. 3a,d), whereas sample MIZ1-08 has a smaller dynamic range. Normalising the dose response data to their maximum signal intensity reduces some of this variability (data not shown) but is not a suitable approach for samples that have not been dosed to saturation. An alternative approach is to normalise the curves by a particular dose, here arbitrarily selected as 1,442 Gy (7,000 s of irradiation) which is the maximum common dose for most aliquots measured in this study. Unfortunately, as sample MIZ1-08 has a D_e > 1,442 Gy it is not possible to include the SAAD measurement of this sample in the SGC. Normalisation reduces variability between the SAAD dose response curves (Fig. 3b,e) and allows development of a common SGC for all samples (Fig. 3c,f), irrespective of measurement protocol, i.e. SAR or SAAD, with or without preheat.

The SGCs for the Al- and Ti-centres can be well described with either a DSE or SSE (Fig. 3c,f, Fig. S6) fitted to the maximum ESR intensities (i.e., I_{max}) without data weighting. Contrasting D_e values computed using individual dose response curves and the SGCs shows good agreement for the different Ti-centres, with almost all D_e values within 25 % of one another. However, the Al-centre exhibits greater variability with most SGC D_e values overestimating D_e values obtained from individual sample fitting by >25 %. This discrepancy reflects a mismatch between model fit and dose response curve shape caused by fitting the full dose response curve into saturation. Where D_e values are instead calculated from linear interpolation between datapoints

https://doi.org/10.5194/egusphere-2026-2204
Preprint. Discussion started: 23 April 2026

using the SGC, or where the SGC is truncated to an arbitrarily selected maximum dose of 4.5 kGy before fitting, the deviation reduces to <15 % for most samples. Saturation levels estimated from $2D_0$ and assuming an environmental dose rate of 6 Gy ka^{-1} are ~1.2 Ma for the Ti-centre and ~10 Ma for the Al-centre.

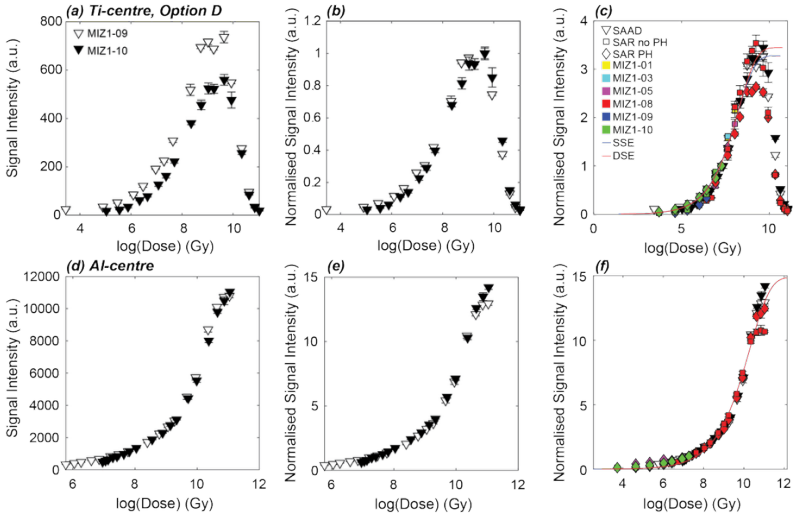

Figure 3: SAAD and SAR dose response curves. (a,d) Non-normalised SAAD data for samples MIZ1-09 and MIZ1-10 for the Ti- and Al-centres respectively, (b,e) SAAD data normalised by an arbitrary dose of 1,442 Gy for the Ti- and Al-centres respectively, and (c,f) SAAD and SAR data for all samples, normalised by an arbitrary dose of 1,442 Gy for the Ti- and Al-centres respectively. Standardised growth curve data fits are shown in panels c and f.

ESR-thermochronometry calculations are usually done using the fraction of occupied traps, which means that it is essential to characterise dose response curves into saturation. Although the SGCs developed here lead to some mismatch in D_e values, relative to sample specific dose response curves, this will not necessarily affect n/N values, which are simply the ratio between the maximum possible ESR intensity (N) and the natural signal intensity (n) as quartz ESR is not affected by anomalous fading (see discussion in Valla et al., 2016 for the implications on n/N for feldspar OSL-thermochronometry). The fraction of electron trap filling was calculated for all samples using the SGCs and an SSE fit. A reduction in n/N values with increasing borehole temperature is observed (Fig. 1b,d), consistent with the trend in signal intensity with temperature (Fig. 1a,c).

4.2 Thermal Stability

The thermal stability of the different samples was measured using an isothermal holding experiment. All samples except MIZ1-08 exhibited similar thermal stability, and the data could be combined and fitted well using the Gauss model (Lambert, 2018; King et al., 2020) to derive a single set of kinetic parameters for both the Al and Ti-centres (Table 1, Fig. 4). The lifetimes of the centres investigated are sufficiently stable for dating over ~1 Ma for the Ti-centre and ~10 Ma for the Al-centre.

https://doi.org/10.5194/egusphere-2026-2204
Preprint. Discussion started: 23 April 2026

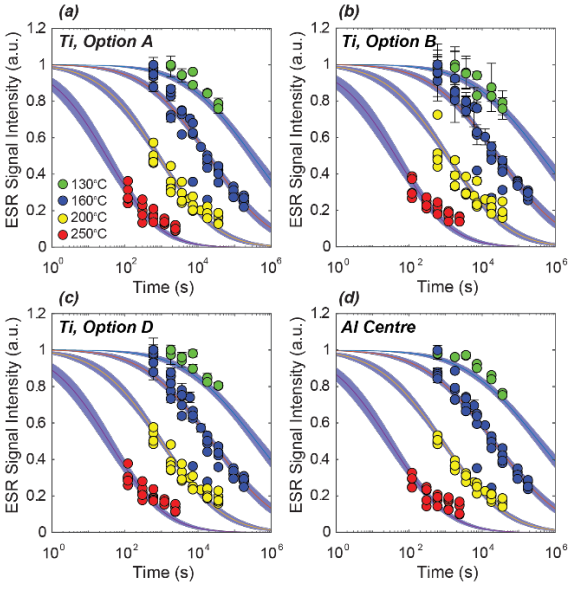

225 **Fig. 4: Combined isothermal decay data from all samples except MIZ1-08 which displayed different thermal kinetic parameters. Data are fitted using the Gauss model (Lambert, 2018; King et al., 2020).**

4.3 Data inversion

In a first step, each of the samples were inverted separately for borehole temperature using an approach modified from Guralnik et al. (2015). Signal accumulation and loss were modelled using the SGC n/N and D_0 values and common thermal kinetic
230 parameters (Table 1) assuming single-saturating exponential growth and Gaussian thermal decay (King et al., 2020). Kinetic parameters were randomly sampled, accounting for covariance, and were used to model n/N values for 160 different isothermal histories over 40 Ma with temperatures between 0 and 80 ºC. Modelled n/N values were contrasted with the SGC n/N values for each ESR centre to calculate the likelihood, and these results were then filtered using a rejection algorithm (see King et al., 2016 and King et al., 2020 for full details of the inverse method). Whereas the Al-centre data yield inverted temperatures that
235 are generally within 1σ uncertainty of the modern-day borehole temperature, the Ti-centre (Option D) data yield temperatures much greater than the modern-day borehole temperature, with an offset of up to 30 ºC (Fig. 5).

https://doi.org/10.5194/egusphere-2026-2204
Preprint. Discussion started: 23 April 2026

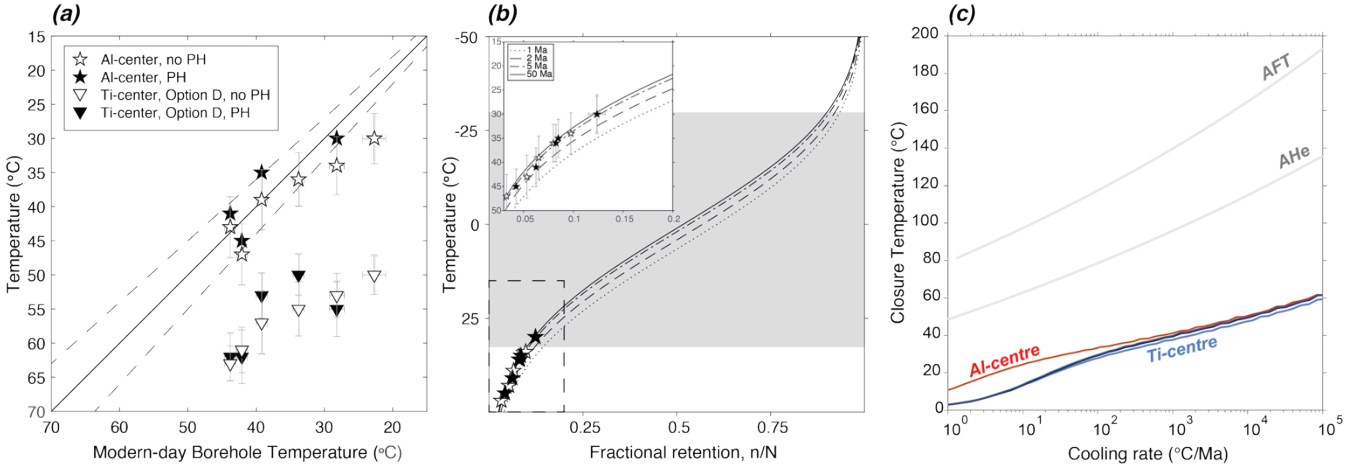

Figure 5: Individual sample temperature inversion results for (a) the Al-centre and Ti-centre (Option D) relative to modern-day borehole temperature (Uozumi et al., 2005). The dashed lines show 10% deviation from the 1:1 line. (b) Inverted temperatures for the Al-centre plotted relative to the partial retention zone (grey shaded area). The fractional signal retention for the Al-centre is predicted assuming isothermal conditions for 1, 2, 5 and 50 Ma. (c) Closure temperature for different cooling rates for the Al- and Ti-centre signals calculated using the average kinetic parameters in comparison with the apatite fission-track (AFT) and apatite helium (AHe) thermochronometric systems calculated using kinetics from Ketcham et al., (1999) and Farley (2000) respectively. The different Ti-centre options are shown in different shades of blue but are almost indistinguishable.

In a second step, the samples were inverted together as a vertical profile by using their relative depth in the borehole and a geothermal gradient. As sample MIZ1-01 has depth of only 159 m (Table 1) and is within a zone where surface temperature changes and fluid circulation (Uozumi et al., 2005) may influence borehole temperature, this sample was excluded from these inversions. Temperature histories of sample MIZ1-03 (top sample of the vertical profile) were randomly generated before a geothermal gradient of 19 ± 2 °C was used to estimate the temperature of the deeper borehole samples. As the Al-centre and Ti-centre (Option D) reach their signal steady-state with present-day borehole temperature in about 10 and 1 Myr, we consider cooling history simulation times of 30 and 3 Myr respectively, corresponding to three times their equilibrium time to ensure all cooling histories potentially recorded by the centres are considered. Rather than imposing isothermal conditions, thermal histories were allowed to cool monotonically but were constrained to be <100 °C, a limit imposed by the AFT ages greater than 40 Ma (Yuguchi et al., 2017, AFT closure temperature 100-120°C), and to within 10 °C of the present-day temperature of sample MIZ1-03 (28.2 °C). For each cooling history, kinetic parameters were sampled and the same rejection algorithm applied as in the previous inversion. Whereas inverting the Al-centre data yielded temperatures commensurate with the measured borehole temperatures and indicated thermal steady-state for at least 5-10 Ma, inversion of the Ti-centre (Option D) resulted in overestimation of the borehole temperature by 15-30 °C within the last 1 Myr (Fig. 6h-i). Inverting both the Al- and Ti-centre (Option D) data together reduces this discrepancy but still overestimates borehole temperature by 2-10 °C (Fig. 6j).

https://doi.org/10.5194/egusphere-2026-2204
Preprint. Discussion started: 23 April 2026

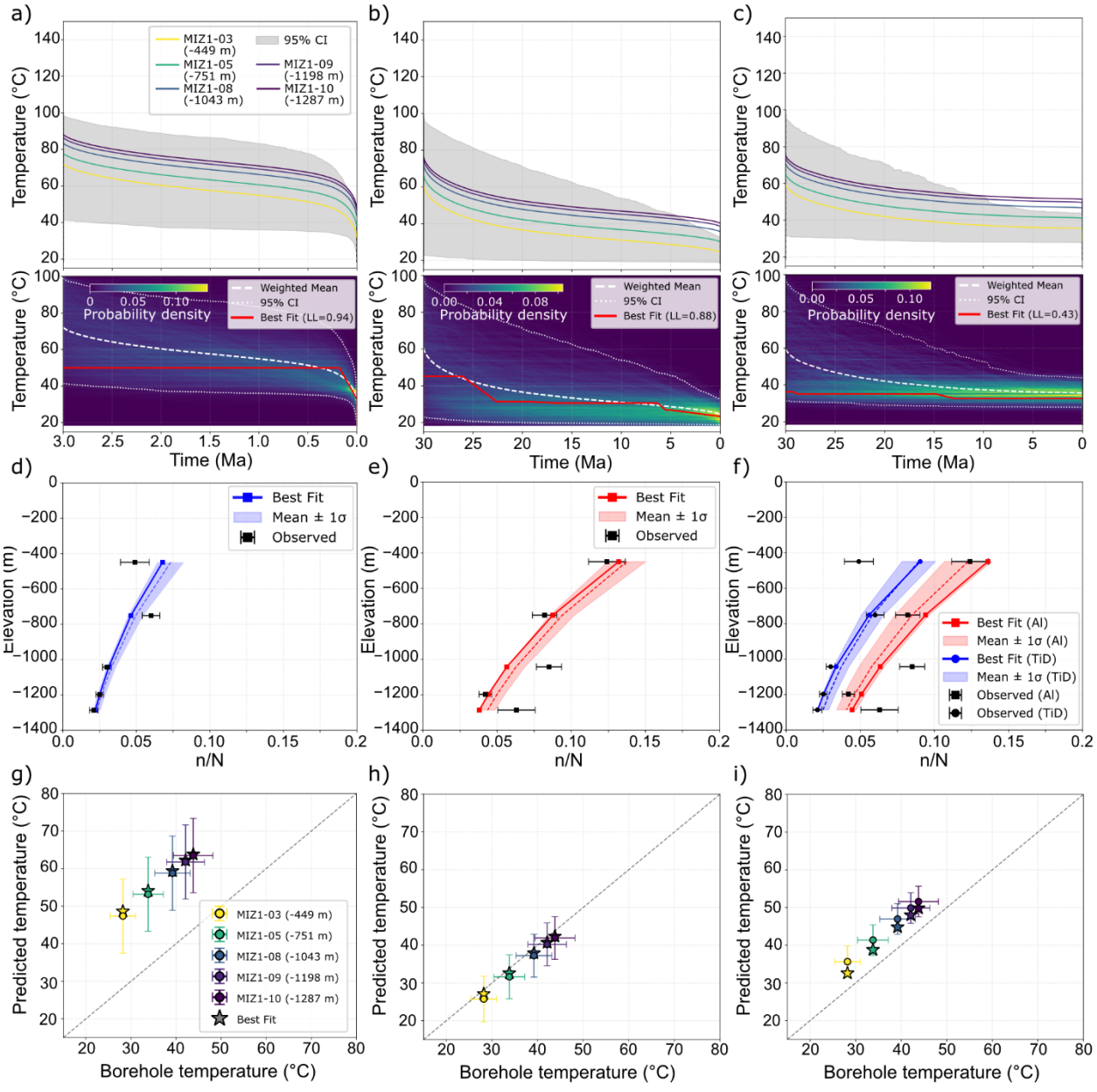

Figure 6: Vertical profile inversion results for the Al-centre and Ti-centre (Option D). Inversion of the Ti-centre (Option D) is shown in the left column, the Al-centre in the central column and both centres together in the right column. (a-c) Inverted thermal histories. The weighted mean paths for each sample are shown on the top panels with the grey shaded area corresponding to the 95% credible interval of accepted path for the top sample (MIZ1-03). The bottom panels show the density distribution of accepted cooling histories (LL refers to Log-Likelihood). (d-f) Measured and modelled n/N values with borehole depth for the different samples. (g-i) Observed vs predicted temperatures for

https://doi.org/10.5194/egusphere-2026-2204
Preprint. Discussion started: 23 April 2026

the different samples (note that as the same geothermal gradient is used between samples, they are perfectly correlated with one another).

To explore the potential cause of the Ti-centre (Option D) temperature discrepancy, relative to measured borehole temperatures, we contrasted the prior and posterior distributions of the kinetic parameters retained by the inverse model. To fit both the Al and Ti-centre (Option D) data, only the extremes of the prior distribution were retained (Fig. S8). This is unsurprising as the kinetic parameters of the Al and Ti-centre (Option D) are similar (Table 1), but they predict very different thermal histories (Fig. 5a). The median posterior Ti-centre (Option D) distribution indicates $\mu(E_t)$ of 1.32 ± 0.04 eV, $\sigma(E_t)$ of 0.108 ± 0.005 eV, log10(s) of 10.8 ± 0.43 s^{-1}, relative to prior values of 1.41 ± 0.05 eV, 0.120 ± 0.013 eV and 11.8 ± 0.53 s^{-1} (Table 1, Fig. S8). To evaluate whether these posterior kinetic parameters could be correct, we contrasted the goodness of fit of the isothermal decay data using the prior and median posterior values; the prior values exhibited a better fit although the difference in the quality of fit was small (BIC of -646.2 and -616.2 for the prior and median posterior kinetic parameters respectively, Fig. S9). The main difference is found for the tail of the isothermal decay curves for which the posterior kinetic predict faster signal decrease than observed for similar holding time and temperature (Fig. S9).

An alternative explanation for the mismatch between the Ti-centre (Option D) data and borehole temperature is that the dose response curve of the Ti-centre (Option D) was not accurately constrained, possibly because of dose quenching which is commonly reported to affect Ti-centre dose response (e.g. Woda and Wagner, 2007; Figs. 2 and 3). Because n/N is calculated relative to the saturation level of the dose response curve, D_0 and n/N are directly correlated: an overestimation of D_0 will result in an underestimation of n/N and vice versa. We ran a final inversion whereby the borehole temperatures and the thermal kinetic parameters were fixed (Table 1) and instead allowed D_0 to vary between 1000 and 4000 Gy. We computed a revised n/N value for each corresponding D_0 and found that a D_0 value of 2740 ± 174 Gy and n/N values ~0.1 greater would yield temperatures commensurate with borehole temperature (Fig. S10). However, examination of the dose response curve data and fit (Fig. 3c) does not suggest that D_0 was overestimated, unless the preheated SAR data of sample MIZ1-08 are considered more representative than SAAD measurements of samples MIZ1-09 and MIZ1-10 and the non-preheated SAR data of sample MIZ1-08.

Finally, the closure temperature of the Ti-centre and Al-centre were calculated using an equation modified from Guralnik et al. (2013). The greater D_0 value of the Al-centre increases its closure temperature slightly for lower cooling rates, in comparison to the Ti-centre, and for these samples, both the Al and Ti-centres yield closure temperatures significantly lower than the AHe and AFT systems shown for comparison in Fig. 5c.

https://doi.org/10.5194/egusphere-2026-2204
Preprint. Discussion started: 23 April 2026

6 Discussion

The MIZ1 borehole samples exhibited suitable ESR signal properties for measurement of the Al and Ti-centres. Dose-recovery tests and the comparison between SAR and SAAD data indicate that the SAR measurement protocol does not provoke sensitivity changes throughout analysis. As the properties of the majority of the MIZ1 samples are similar, it was possible to construct a standardised growth curve of the data from which the characteristic dose of saturation (D_0) and the fraction of saturation (n/N) could be determined. Whereas the Al-centre could be well described by a SSE or DSE fit, the Ti-centre exhibited sub-linear dose response for both SAR and SAAD measurements (Fig. S2 and S7), which resulted in poor fitting in the dose range of the D_e values (<300 Gy) and thus relatively large D_e value uncertainties (Table S1).

Isothermal decay data from all samples except MIZ1-08 could be combined and fitted to yield a single set of thermal kinetic parameters for the Al and Ti-centres, as has been proposed previously for OSL-thermochronometric studies (Bouscary and King, 2024). This was likely possible due to the similar lithology of the MIZ1 samples, as previous attempts on samples of different lithologies from the same site in the European (Wen et al., 2024) and Japanese Alps (Bartz et al., 2024) were unsuccessful. These common kinetic parameters were used to invert the data for isothermal temperature and rock cooling.

Data inversion for isothermal temperature showed that the Al-centre yielded temperatures that are generally commensurate with modern-day borehole temperature (Fig. 5a). The greatest deviation between modern-day borehole temperature and the inverted temperatures is observed for sample MIZ1-01 which overestimates the modern-day borehole temperature of 22.8 ± 1.7 °C by ~7 °C, although the inverted and modern-day borehole temperatures are within 2σ uncertainties. Sample MIZ1-01 is the shallowest sample (159 m) and as such its temperature is most affected by surface temperature perturbations, that occur seasonally and over longer timescales (e.g. Pollack, 1993; Kohl, 1998; Bodri and Cermak, 2011). Following drilling of the MIZ1 borehole, direct temperature measurements at this depth made in January 2004, July 2004 and September 2004 varied by up to ~3 °C (Uozumi et al., 2015). Fluid circulation was also observed to cause both positive and negative temperature anomalies relative to the measured geothermal gradient of 19 °C (Uozumi et al., 2015). Sample MIZ1-01 is located near to the interface between sedimentary rock and the Tono granite, the change in permeability between the two units likely results in a concentration of fluid flow which may also make this sample location more sensitive to fluid induced temperature fluctuations. A final possible explanation for the temperature deviation could be the effect of rock exhumation. Previous studies indicate that exhumation at the MIZ1 borehole is on the order of 0.11-0.20 mm/yr (Hama et al., 2016) over the past 1 Ma, which assuming a geothermal gradient of 19 °C/km would be equivalent to 2.1-3.8 °C of cooling over the past ~1 Ma. The apparent age of sample MIZ1-01 is 549 ± 67 ka, and thus this sample would have been affected by at least ~1-2 °C of cooling, although note that the apparent age underestimates the time since system closure because of the non-linearity of signal accumulation with rock cooling. The non-preheated aliquot of MIZ1-03 overestimates the modern-day borehole temperature by ~4 °C, however the pre-heated aliquot only overestimates the temperature by ~2 °C and is within 1σ uncertainty. The cause of the

https://doi.org/10.5194/egusphere-2026-2204
Preprint. Discussion started: 23 April 2026

discrepancy between the two aliquots is unclear but may be related to preheating. For the samples taken from deeper in the borehole, the individual sample inverted temperatures agree well with the modern-day borehole temperature. If sample MIZ1-01 is excluded, a geothermal gradient of 14 °C/km is obtained from the individual sample inverted temperatures and depths of the remaining samples (Fig. 5a). This geothermal gradient is lower than the modern-day measured value of 19 °C/km, however, where the Al-centre of all samples excluding MIZ1-01 are inverted together, it is possible to fit the data assuming a geothermal gradient of 19 °C/km (Fig. 6). This suggests that the mismatch observed when samples are inverted individually could be related to sample uncertainties, or to the simplistic isothermal model set-up, rather than sensitivity of the ESR system to the low rate of exhumation at this locality (~0.11-0.20 mm/yr), which would act to suppress the apparent geothermal gradient for thermochronometric systems that average temperature-change over kyr-Myr timescales.

The broad agreement between the ESR-thermochronometry data and modern-day borehole temperatures is highly encouraging and provides the first robust field validation of the ESR-thermochronometry technique. Whilst previous measurements of samples from the KTB borehole, Germany (Scherer et al., 1993) and Fergusons Hill-1 borehole from the Otway Basin, Australia (Fang and Grün, 2020) have shown that ESR signals reduce with increasing borehole temperature, these studies did not determine the thermal kinetic parameters from laboratory experiments. The ability to accurately constrain thermal kinetic parameters for samples independent of their stratigraphic context is essential for rock exhumation applications (e.g. Wen et al., 2024).

In contrast, all options for the Ti-centre overestimate the current ambient temperature of the MIZ1 borehole (Fig. 5a). These data have similar thermal stability to the Al-centre and more than 1 km of exhumation within the past 1 Myr would be needed to explain their thermal anomaly, which is implausible given the existing geological evidence. The overestimation of temperature from the different options of the Ti-centre could be related either to an underestimation of natural n/N values, or alternatively to overestimation of the thermal stability of the Ti-centre. The latter option seems unlikely given the fit to the experimental data (Fig. S9) and that the kinetic parameters obtained are within the range of previously reported values (see Fang and Grün, 2020 for a summary). Similarly, given their similar thermal stability (Table 1, Fig. 6), it is not plausible that the Ti-centre is able to detect a rock cooling signal (e.g. from exhumation) that the Al-centre would not also be sensitive to. Assuming that the thermal kinetic parameters are correct, rather the natural n/N signals may be underestimated, possibly related to overestimation of D_0, although this is not evident from the dose response curve data (Fig. 3c). The Ti-centre dose response curves are sub-linear (Fig. S2), and contrast with data measured for other rock samples using the same methodological approach (e.g. Bartz et al., 2024; Wen et al., 2024). As the quality control checks made for the Ti-centre (dose-recovery test, comparison of SAR and SAAD dose response curve shape) imply that the signals investigated are reliable, the underestimation of natural n/N values may relate to irradiation or heating-induced sensitivity change throughout measurement, that could not be successfully monitored. A validation study for the Ti-centre is thus urgently needed, to demonstrate the reliability of Ti-centre ESR thermochronometry data.

https://doi.org/10.5194/egusphere-2026-2204
Preprint. Discussion started: 23 April 2026

Ogata et al. (2022) previously used OSL-thermochronometry to investigate the MIZ1 borehole. They recorded OSL apparent ages of ~100 ka for the different samples, that were in thermal equilibrium with borehole temperature. Forward modelling of their data together with the ESR data from this study (Fig. S11) shows that the ESR centres have a lower closure temperature than the OSL signals for these samples. Whereas the OSL signals begin to accumulate charge at ~100 °C, the ESR signals begin to accumulate at ~60 °C for a cooling rate of 10 °C Myr^{-1}. The differences in apparent age between the OSL data (~100 ka), Ti-centre (20-30 ka) and Al-centre (90-500 ka) data thus reflect different equilibrium levels between charge trapping and detrapping, linked in part to their different saturation thresholds, and illustrate the difficulty of using apparent age for trapped-charge dating systems.

7 Conclusion

ESR thermochronometry was successfully applied to six samples from the MIZ1 borehole. Inversion of the Al-centre data yielded temperatures commensurate with modern-day borehole temperature for all samples except MIZ1-01 which has depth of 159 m. Surface temperature variability, fluid flow and potentially temperature changes driven by exhumation likely explain this discrepancy. In contrast, the different Ti-centre options overestimated borehole temperature by >15 °C, which is likely related to sub-linearity observed in the measured dose response curves or to sensitivity changes that were not detected by data quality tests. An ESR standardised growth curve was developed for the first time for quartz and used to reduce sample measurement times. This is particularly important for thermochronometric investigations where it is necessary to irradiate samples into saturation. Similarly for these samples that are lithologically similar, it was possible to combine isothermal decay data of different samples to obtain a common set of kinetic parameters. In future studies, common kinetic parameters may also offer a means of expediating sample measurement, although this should be evaluated on a site-by-site basis.

Code and data availability

All code and data used for in this study are available from Zenodo (link to be added once revised manuscript has been accepted). In the interim the code and data are available here: https://tinyurl.com/2rmfwkv7

Supplement link

Please add link to supplementary data.

https://doi.org/10.5194/egusphere-2026-2204
Preprint. Discussion started: 23 April 2026

Author contributions

GEK and LB designed the experiments, carried them out and conducted the data analysis with input from MKB and XW. MB, BG and FH contributed to the numerical treatment of the data and MO and SS provided guidance on the geological context of the samples. All co-authors contributed to writing the manuscript.

Competing interests

GK and SS are members of the GChron Editorial board.

Acknowledgements

Katherine Zimmerman is thanked for laboratory assistance. Sumiko Tsukamoto is thanked for useful discussions regarding the data. We are grateful to an anonymous reviewer whose feedback improved the manuscript.

Financial support

This research was supported by funding from the European Research Commission (ERC) under the European Union's Horizon 2020 research and innovation programme, grant number 851614.

Review statement

References

Bartz, M., King, G.E., Bernard, M., Herman, F., Wen, X., Sueoka, S., Tsukamoto, S., Braun, J., Tagami, T.: The impact of climate on relief in the northern Japanese Alps within the past 1 Myr – the case of the Tateyama mountains. Earth and Planetary Science Reviews 644, 118830, 2024.

Bell, W.T.: Alpha dose attenuation in quartz grains for thermoluminescence dating. Ancient Tl, 4(3), pp.4-8, 1980.

Bodri, L. and Cermak, V.: *Borehole climatology: a new method how to reconstruct climate*. Elsevier, 2011.

Bossin, L., King, G.E.: Constraining heterogeneity in the absorbed dose of 50 keV X-ray irradiated samples for EPR dating: simulation and experimental approaches. AncientTL 39(2), pp.1-11, 2021.

Bouscary, C. and King, G.E.: Exploring the use of averaged thermal kinetic parameters in luminescence thermochronology. Radiation Measurements, p.107215, 2024.

Durcan, J.A., King, G.E. and Duller, G.A.: DRAC: Dose Rate and Age Calculator for trapped charge dating. Quaternary Geochronology, 28, pp.54-61, 2015.

https://doi.org/10.5194/egusphere-2026-2204
Preprint. Discussion started: 23 April 2026

Duval, M. and Guilarte, V.: ESR dosimetry of optically bleached quartz grains extracted from Plio-Quaternary sediment: evaluating some key aspects of the ESR signals associated to the Ti-centers. Radiation Measurements, 78, pp.28-41, 2015.

Fang, F. and Grün, R.: ESR thermochronometry of Al and Ti centres in quartz: A case study of the Fergusons Hill-1 borehole from the Otway Basin, Australia. Radiation Measurements, 139, p.106447, 2020.

Farley, K.A.: Helium diffusion from apatite: General behavior as illustrated by Durango fluorapatite. Journal of Geophysical Research: Solid Earth, 105(B2), pp.2903-2914, 2000.

Grün, R., Tani, A., Gurbanov, A., Koshchug, D., Williams, I., & Braun, J.: A new method for the estimation of cooling and denudation rates using paramagnetic centers in quartz: A case study on the Eldzhurtinskiy Granite, Caucasus. Journal of Geophysical Research: Solid Earth, 104(B8), 17531-17549, 1999.

Guérin, G., Mercier, N. and Adamiec, G.: Dose-rate conversion factors: update. Ancient Tl, 29(1), pp.5-8, 2011.

Guérin, G., Mercier, N., Nathan, R., Adamiec, G. and Lefrais, Y.: On the use of the infinite matrix assumption and associated concepts: a critical review. Radiation Measurements, 47(9), pp.778-785, 2012.

Guralnik, B., Jain, M., Herman, F., Paris, R.B., Harrison, T.M., Murray, A.S., Valla, P.G. and Rhodes, E.J.: Effective closure temperature in leaky and/or saturating thermochronometers. Earth and Planetary Science Letters, 384, pp.209-218, 2013.

Hama, K., Sasao, E., Iwatsuki, T., Onoe, H., Sato, T., Yasue, K., Asamori, K., Niwa, M., Osawa, H., Nagae, I. and Natsuyama, R.: Synthesized research report in the second mid-term research phase. Mizunami Underground Research Laboratory project, Horonobe Underground Research Laboratory project and geo-stability project (Translated document) (No. JAEA-REVIEW--2016-014). Japan Atomic Energy Agency, 2016.

Ketcham, R.A., Donelick, R.A. and Carlson, W.D.: Variability of apatite fission-track annealing kinetics: III. Extrapolation to geological time scales. American Mineralogist, 84(9), pp.1235-1255, 1999.

King, G.E., Herman, F. and Guralnik, B.: Northward migration of the eastern Himalayan syntaxis revealed by OSL thermochronometry. Science, 353(6301), pp.800-804, 2016.

King, G.E., Tsukamoto, S., Herman, F., Biswas, R.H., Sueoka, S. and Tagami, T.: Electron spin resonance (ESR) thermochronometry of the Hida range of the Japanese Alps: validation and future potential. Geochronology, 2(1), pp.1-15, 2020.

Kohl, T.: Palaeoclimatic temperature signals—can they be washed out?. *Tectonophysics*, *291*(1-4), pp.225-234, 1998.

Kuwahara, T.: The Noobi Basin and its fault block movements. The Quaternary Research (Daiyonki-Kenkyu), 7(4), pp.235-247, 1968.

Lambert, R.: Investigating thermal decay in K-feldspar for the application of IRSL thermochronometry on the Mont Blanc massif, Unpublished PhD Thesis, University of Lausanne, Switzerland, 2018.

Moriyama, A. and Niwa, M.: Some problems on the formation of Toki surface (Early Pleistocene) in Tono district and northwestern Mikawa Plateau, central Japan. Geogr. Rev. Jpn, 58, pp.275-294, 1985.

https://doi.org/10.5194/egusphere-2026-2204
Preprint. Discussion started: 23 April 2026

Ogata, M., King, G.E., Herman, F. and Sueoka, S.: Reconstructing the thermal structure of shallow crust in the Tono region using multi-OSL-thermometry of K-feldspar from deep borehole core. Earth and Planetary Science Letters, 591, p.117607, 2022.

Pollack, H.N.: Climate change inferred from borehole temperatures. *Global and planetary change*, *7*(1-3), pp.173-179, 1993.

Preusser, F., Chithambo, M.L., Götte, T., Martini, M., Ramseyer, K., Sendezera, E.J., Susino, G.J. and Wintle, A.G.: Quartz as a natural luminescence dosimeter. Earth-Science Reviews, 97(1-4), pp.184-214, 2009.

Scherer, T., Agel, A., Hafner S.S., Determination of uplift rates using ESR investigations of quartz, KTB Rep. 93-2. Kontinentales Tiefbohrprogram der Bundesrepublic Deutschland Niedersächs. Landesamt Bodenforsch., Hannover, 121- 124, 1993.

Tajikara, M., Yasue, K.N.I., Yanagida, M., Furusawa, A., Tanaka, N., Morita, Y. and Sugai, T.: Fluvial terrace and geomorphology in the Tokigawa (Shonaigawa) River basin since the middle Pleistocene. Geographical Review of Japan, 84(2), pp.118-130, 2011.

Toyoda, S. and Falguères, C.: The method to represent the ESR signal intensity of the aluminium hole center in quartz for the purpose of dating. Advances in ESR applications, 20, pp.7-10, 2003.

Tsukamoto, S., Toyoda, S., Tani, A. and Oppermann, F.: Single aliquot regenerative dose method for ESR dating using X-ray irradiation and preheat. Radiation Measurements, 81, pp.9-15, 2015.

Uozumi, N., Murakami, S., Oishi, Y. and Kawamura, H.: Drilling Investigations in Mizunami Underground Research Laboratory Project. Japan Nuclear Cycle Development Institute Report TJ7440, pp.2005-2091, 2005.

Valla, P.G., Lowick, S.E., Herman, F., Champagnac, J.D., Steer, P. and Guralnik, B.: Exploring IRSL50 fading variability in bedrock feldspars and implications for OSL thermochronometry. Quaternary Geochronology, 36, pp.55-66, 2016.

Wen, X., Bartz, M., Schmidt, C., King, G.E.: ESR and Luminescence thermochronometry of the Rhône valley, Switzerland. Quaternary Geochronology, 2024.

Woda, C. and Wagner, G.A.: Non-monotonic dose dependence of the Ge-and Ti-centres in quartz. Radiation measurements, 42(9), pp.1441-1452, 2007.

Wu, T.S., Jain, M., Guralnik, B., Murray, A.S. and Chen, Y.G.: Luminescence characteristics of quartz from Hsuehshan Range (Central Taiwan) and implications for thermochronometry. Radiation Measurements, 81, pp.104-109, 2015.

Yuguchi, T., Sueoka, S., Iwano, H., Izumino, Y., Ishibashi, M., Danhara, T., Sasao, E., Hirata, T. and Nishiyama, T.: Position-by-position cooling paths within the Toki granite, central Japan: Constraints and the relation with fracture population in a pluton. Journal of Asian Earth Sciences, 169, pp.47-66, 2019.